EFFECT OF HEAT EXCHANGER FLOW PROCESSES ON THE PHASE CHANGE COOLING SYSTEM OF VEHICLE FUEL CELLS

by

Jing BAI*, Mingzhi CHEN, Siqi CUI, Huifang FAN, Siyuan HE, Lejian WANG, Huixin LI, Cheng LI, and Kexuan GU

School of Smart Energy and Environment, Zhongyuan University of Technology, Zhengzhou, China

Original scientific paper
https://doi.org/10.2298/TSCI2503935B

In response to the issues of high heat dissipation density, large heat generation, and low heat dissipation efficiency of proton exchange membrane fuel cells, this paper develops a vehicle fuel cell heat dissipation performance test bench. The bench employs HFE-7100 phase change cooling fluid and utilizes three distinct configurations of heat exchangers under ambient conditions of 35 °C. The heat dissipation characteristics of the system are then analyzed under varying working fluid-flow rates and fan speeds. The results demonstrate that, when subjected to the same fan speed and working fluid-flow rate, the system with three-process heat exchangers exhibits the most optimal heat dissipation performance. The heat dissipation of the system is observed to be 7% to 16.7% higher than that of the two-process configuration, and 5.1% to 7.2% higher than that of the four-process configuration. Moreover, the energy efficiency ratio of the system ranges from 18.58 to 26.62, indicating a notable reduction in energy consumption when compared to the two-process (3.9% to 10.3% improvement) and the four-process (7.4% to 12.7% improvement).

Key words: *fuel cell, phase change heat dissipation, heat exchanger process, energy efficiency ratio*

Introduction

As the global economy continues to develop at a rapid pace, energy crises [1] and environmental pollution [2] have become increasingly prominent concerns for countries around the world. Achieving low-carbon development and enhancing the utilization of clean energy [3, 4] have emerged as a global consensus, reflecting the growing recognition of the need to address these challenges. In the context of the global energy transition to clean, low-carbon sources, hydrogen energy has emerged as a crucial development opportunity as a clean energy source. The most feasible application of hydrogen energy is in transportation, particularly in vehicles, where it can be converted into clean electric power through fuel cells to serve as a power source. Consequently, in response to both policy and market forces, China has witnessed a surge in the production and sale of new energy vehicles. Hydrogen fuel cells, in particular proton exchange membrane fuel cells (PEMFC) [5], exhibit high energy conversion efficiency, a wide operating range, convenient and rapid fuel replenishment, and pollu-

* Corresponding author, e-mail: baijing13703842765@163.com

tion-free emissions. These are devices for the direct conversion of chemical energy into electric energy through electrochemical reactions. In comparison to traditional fuel vehicles, fuel cells possess several advantages, including high energy density, rapid charging, and a wide operating range [6, 7]. These attributes position them as a crucial element in the future of sustainable automotive development [8]. During operation, fuel cells convert approximately 40% to 60% of the chemical energy in the fuel and oxidant into electricity, with the majority of the remaining energy being converted into heat [9]. In the event that the heat is not effectively managed in a timely manner, the internal temperature of the cell will significantly increase, resulting in a pronounced decline in the performance of the stack. Temperature is a crucial factor influencing the performance of fuel cells. It affects not only the transport characteristics of gases, the management of water, and the electrochemical reaction activity, but also the efficiency and stability of the stack [10].

The fuel cell cooling system has been a subject of significant interest among scholars both domestically and internationally. Tong, *et al.* [11] constructed a test platform for a 36 kW fuel cell engine cooling system and developed a set of 3-D fuzzy control rules. The results indicate that the system can ensure the fuel cell operates within the optimal temperature range, with temperature control errors meeting design requirements, and the cooling efficiency satisfying the system cooling needs. Zhao [12] employed a high-efficiency heat exchanger with an isothermal plate for air cooling in PEMFC, which resulted in a significant improvement in temperature uniformity within the cell stack, with a maximum internal temperature difference of only 5.3 ℃. This verifies the viability of implementing isothermal plates in compact air-cooled PEMFC cooling systems. Zheng *et al.* [13] developed a 1-D simulation model for the thermal management system of a vehicle-mounted fuel cell. A sensitivity analysis was conducted on the air-flow rate and outlet water temperature of the cell stack. The results indicate the ability to accurately analyze the outlet water temperature of the cell stack under different operating conditions, enabling precise assessment of the outlet water temperature of the cell stack under various operating conditions. Ding *et al.* [14] developed a computational model for the heat transfer and flow resistance characteristics of radiators using MATLAB. The model was validated through experiments and its cooling effectiveness was compared under different operating conditions for fuel cell system radiators. Tao, *et al.* [15] developed a mathematical model for the auxiliary cooling system of vehicle-mounted PEMFC. The results indicated that when the pump output was 30 Lpm (200 kPa), the three-parallel scheme reduced the pipeline flow resistance by 40.7% compared to the two-parallel scheme. Furthermore, it was found that the addition of a third parallel scheme to the system resulted in a 40.7% reduction in pipeline flow resistance compared to the two-parallel scheme.

A review of the literature on fuel cell cooling systems revealed a paucity of experimental studies on phase-change cooling. In order to address the challenges of high thermal load and high temperature precision requirements in fuel cells, this paper proposes a two-phase cooling method. A compact and high performance parallel flow heat exchanger is selected based on the separated heat pipe technology. A test platform for automotive fuel cell cooling performance was constructed using HFE-7100 as the phase-change working fluid. Phase-change cooling experiments were conducted under three different flow heat exchangers to analyze the cooling characteristics under varying fan speeds and working fluid-flow rates.

Experimental system and working condition

Introduction of experimental equipment

This paper presents the design of an experimental platform for automotive proton exchange membrane fuel cell cooling systems, with a heat dissipation requirement of 15 kW. The schematic diagram of the experimental system circulation is presented in fig. 1. The parameters of each piece of equipment are presented in tab. 1. The layout of the flow channels for the parallel flow heat exchanger is illustrated in tab. 2.

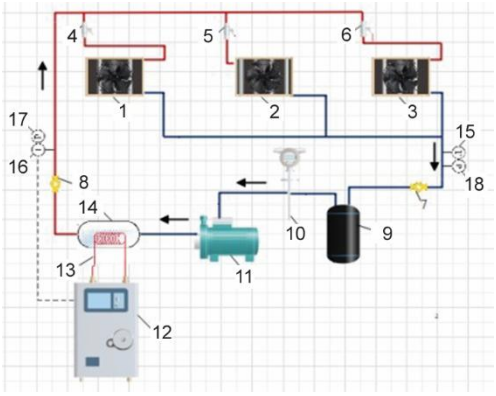

Figure 1. Schematic diagram of heat dissipation system for automotive fuel cell; *1 – two flow processes condenser, 2 – three flow processes condenser, 3 – four [kJkg^{-1}K^{-1}] flow processes condenser; 4, 5, 6 – ball valves, 7, 8 – sight glasses, 9 – liquid storage tank, 10 – mass-flow meter, 11 – water pump, 12 – temperature control box, 13 – electric heating wire, 14 – constant temperature water bath, 15, 16 – temperature sensors, and 17, 18 – pressure sensors*

Table 1. Parameters of each device

Device	Parameter
Condenser	Parallel-flow condenser dimensions: 400 × 352 mm, flat tube height 26 mm, flat tube thickness 1.8 mm
Pump	Model: NP190; motor model: LG8056; nominal flow rate: 1.9 mL/rev, rated flow rate: 5.4 Lpm at 3000 rpm rated head: 15 m, motor power: 800 W, dimensions: 80 × 118 mm
Air blower	WSLNF-261WX-5-10; fan speed: 3150 rpm, air volume: 2500 m³/h, power: 150 W
Temperature sensor	Model: XMTG-6000, measurement precision: ±0.5℃
Pressure sensor	Measurement precision: ±0.5% kPa
Paperless recorder	KSA series 4.3-inch 12-channel
Mass-flow meter	Measurement precision: ±0.2% kg/h
Temperature controller	XMTG-6000

Table 2. Non-symmetric flow passage arrangement

Processes	Tubes	Non-symmetric parameter
2	34	22-12
3		16-12-6
4		12-10-8-4

System principles and calculations

The boiling point of the HFE-7100 working fluid is 61 ℃ at standard atmospheric pressure. The cooling fluid absorbs heat and boils within the cooling plates, thereby maintaining the internal temperature of the cell stack between 60-80 ℃. The vaporized working fluid generated at the heating end is introduced into the heat exchanger, where it begins to flow and undergoes forced convective cooling with the ambient air. The condensed cooling fluid exits the heat exchanger in the form of droplets due to the influence of liquid tension.

The heat dissipation of the heat exchanger:

$$\phi = KA\Delta T_{\mathrm{m}} \tag{1}$$

$$\Delta T_{\mathrm{m}} = \frac{(T_1 - t_2) - (T_2 - t_1)}{\ln \dfrac{T_1 - t_2}{T_2 - t_1}} \tag{2}$$

where ϕ [kW] is the heat dissipation, K [$\mathrm{Wm^{-2}K^{-1}}$] – the overall heat transfer coefficient, A [$\mathrm{m^2}$] – the heat transfer area, ΔT_{m} [K] – the logarithmic mean temperature difference, T_1 [K] – the temperature at the hot fluid inlet, T_2 [K] – the temperature at the hot fluid outlet, t_1 [K] – the temperature at the cold fluid inlet, and t_2 [K] – the temperature at the cold fluid outlet.

When the coolant is utilized in the cooling system, it undergoes cooling through subcooling and phase change heat absorption, and then transfers heat to the environment through the heat exchanger, thereby completing phase change cooling and subcooling cooling. Among these processes, phase change heat dissipation represents the primary mode of heat dissipation. The cooling process itself is responsible for the dissipation of heat.

$$\phi_{\mathrm{cool}} = \phi_{\mathrm{Pha}} + \phi_{\mathrm{sen}} \tag{3}$$

$$\phi_{\mathrm{Pha}} = m\Delta h \tag{4}$$

$$\phi_{\mathrm{Sen}} = C_p m\Delta T \tag{5}$$

where m [$\mathrm{kgs^{-1}}$] is the mass-flow rate of the cooling medium, Δh [$\mathrm{kJkg^{-1}}$] – the latent heat of vaporization of the cooling medium, C_p [$\mathrm{kJkg^{-1}K^{-1}}$] – the specific heat capacity of the liquid phase of the cooling medium, and ΔT [K] – the subcooling of the cooling medium.

The EER indicates the system energy efficiency, representing the efficiency of energy conversion. A higher EER indicates better energy-saving performance of the system. The calculation formula for EER:

$$EER = \frac{\phi}{P} \tag{6}$$

$$P = P_1 + P_2 \tag{6}$$

where P [kW] is the total power consumed during system operation, P_1 [kW] – the power of the water pump, and P_2 [kW] – the power of the fan.

Experimental working conditions

This experiment was conducted in the Standard Enthalpy Difference Laboratory, with the outdoor temperature set at 35 ℃. The experimental conditions are shown in tab. 3.

Table 3. Experimental working conditions

Exchanger process	Outdoor temperature [°C]	Fluid-flow [Lpm]	Fan speed percentage
2 3 4	35	3	20%
		3.5	40%
		4	60%
		4.5	80%

Analysis of experimental results

The heat dissipation characteristics at different fan speed

The fan speeds were set at 20%, 40%, 60%, and 80% of maximum capacity, corresponding to air-flow velocities of 1.6 m/s, 2.3 m/s, 3.4 m/s, and 4 m/s, respectively. The coolant flow rate was maintained at 4 Lpm.

As illustrated in fig. 2(a), the system heat dissipation exhibits a biphasic response to the increase in the number of heat exchanger processes at a constant fan speed. The heat dissipation is greatest at three processes, with heat dissipation values of 14.31 kW, 15.26 kW, 16.21 kW, and 16.51 kW at fan speed percentages of 20%, 40%, 60%, and 80%, respectively. In comparison to two processes, the increase is 14%, 13.7%, 10%, and 9%, respectively. In comparison to four processes, the increase was 5.1%, 7.1%, 6.7%, and 7.1%, respectively. The reason for this is that during the transition from two to three processes in the heat exchanger, the number of processes increases, the flow velocity of the working fluid inside the heat exchanger becomes larger and more evenly distributed, resulting in more sufficient heat dissipation and thereby an increase in heat dissipation. During the transition from three to four processes in the heat exchanger, there is a discernible decline in heat dissipation. This is due to the fact that the structure of the four-process heat exchanger is more complex, resulting in greater flow resistance and an increase in system pressure drop, which consequently affects system heat dissipation.

As illustrated in fig. 2(b), at a constant number of processes in the heat exchanger, an increase in fan speed results in a gradual rise in system power. The energy efficiency of the system must be evaluated in terms of its system EER. As illustrated in fig. 2(c), the pattern of EER under varying fan speeds and heat exchanger process numbers exhibits variability. The

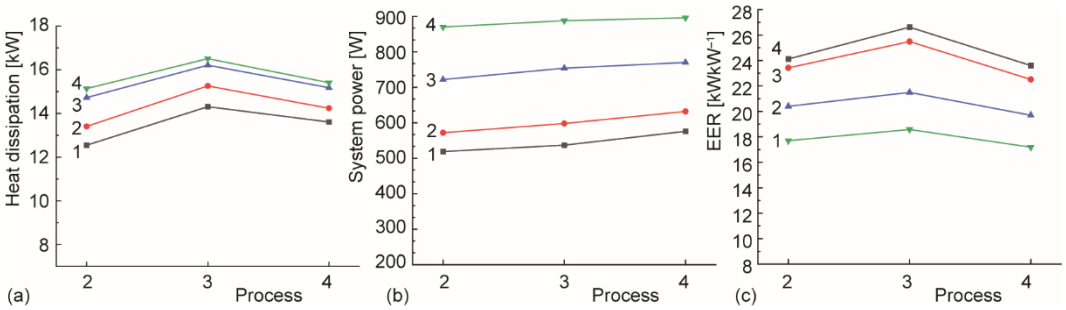

Figure 2. (a) Variation of heat dissipation by fan wind speed for different processes, (b) variation of system power for different processes with fan air speeds, and (c) EER variation of fan wind speed for different processes; *1 – fan percentage 20%, 2 – fan percentage 40%, 3 – fan percentage 60%, and 4 – fan percentage 80%*

EER at a constant fan air-flow velocity is analogous to the trend of system heat dissipation, which exhibits an initial increase with the number of heat exchanger processes and then a subsequent decline. For instance, with three processes, the EER reaches 26.62, 25.49, 21.49, and 18.58 as the fan speed percentage increases, representing respective increases of 10.3%, 8.8%, 5.3%, and 4.9% in comparison to two processes, and increases of 12.7%, 13.2%, 9%, and 8% in comparison to four processes. The primary reason for this phenomenon is the substantial influence of heat dissipation, despite the relatively stable system power. However, the EER for four processes decreases by 2.1%, 3.8%, 3.4%, and 2.8% in comparison to two processes as the fan speed percentage increases. This is because the heat dissipation between the two sets of processes is comparable, but the system power for the four-process configuration is greater, resulting in a reduction in the system EER. Moreover, at the same number of processes, the trend of decreasing system EER becomes more pronounced as the percentage of fan speed increases. This is primarily due to the significant influence of fan power.

The heat dissipation characteristics at different fluid-flow rates

To assess the efficacy of the fuel cell cooling system in dissipating heat, a series of performance tests were conducted at varying fluid-flow rates (3 Lpm, 3.5 Lpm, 4 Lpm, and 4.5 Lpm) and fan speed percentages (60%) with a wind speed of 3.4 m/s.

The variation in system heat dissipation with different fluid-flow rates and heat exchanger process arrangements is illustrated in fig. 3(a). From the figure, it can be observed that at a constant flow rate, the system heat dissipation initially increases and then decreases with an increase in the number of heat exchanger processes. The heat dissipation is highest at three processes, with system heat dissipation reaching 13.8 kW, 15.23 kW, 16.21 kW, and 16.63 kW, respectively, for fluid-flow rates of 3 Lpm, 3.5 Lpm, 4 Lpm, and 4.5 Lpm. This represents a 16.7%, 10.6%, 10.1%, and 7% increase over the heat dissipation of two processes, and a 7.2%, 5.6%, 6.7%, and 5% increase over the heat dissipation of four processes. The number of processes affects heat dissipation. As the number of processes increases, the structure becomes more complex, and some fluid does not completely dissipate heat. As the fluid-flow rate increases, the rate of increase in system heat dissipation decreases in proportion to the heat exchanger processes.

Figure 3(b) illustrates the trend of system power changing in relation to fluid-flow rate and heat exchanger process number. At a constant fluid-flow rate, the power output increases with an increase in the number of heat exchanger processes. The EER is defined as the ratio of energy conversion efficiency. As illustrated in fig. 3(c), the fluctuating trend of the

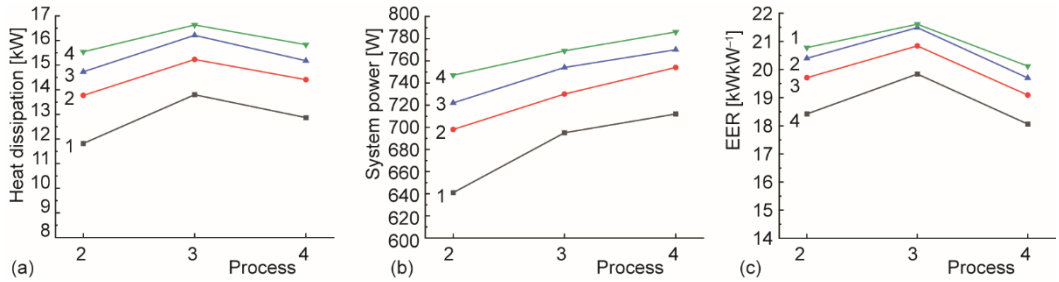

Figure 3. (a) Variation of heat dissipation by work mass-flow rate for different processes, (b) variation of system power for different processes with work mass-flow rate, and (c) variation of EER for work mass-flow rate for different processes; *1 – flow rates 3 L per minute, 2 – flow rates 3.5 Lpm , 3 – flow rates 4 Lpm , and 4 – flow rates 4.5 Lpm*

EER can be employed to ascertain the energy-saving efficacy of the system. From the figure, it can be observed that the EER is at its highest with three processes. As the fluid-flow rate increases, the system efficiency ratio also rises, reaching 19.84, 20.84, 21.49, and 21.61, respectively. These values are 7.7%, 5.7%, 5.3%, and 3.9% higher than that of two processes, and 9.8%, 9.1%, 9%, and 7.4% higher than that of four processes. As the fluid-flow rate increases, the EER also rises, however, the rate of increase in EER diminishes with an increase in flow rate. This phenomenon can be attributed to the influence of heat dissipation, which causes an increase in the flow rate of the working medium and, consequently, an increase in heat dissipation. As the flow rate increases to a certain extent, the working medium is unable to fully exchange heat with the heat exchanger, resulting in a slower increase in heat dissipation. Consequently, the system power increases gradually, while the rate of increase of the system EER slows. The EER of the four-process system is observed to decrease by 6.8% to 8.9% in comparison to the three-process system. This is attributed to the increased number of heat exchanger processes, which leads to a more complex structure, higher system energy consumption, and a decrease in heat dissipation.

Conclusions

The objective of this study was to investigate the heat dissipation characteristics of a fuel cell using HFE-7100 phase-change coolant with a heat dissipation rate of 15 kW. The following conclusions were drawn.

- At a constant fan speed and a fixed working fluid-flow rate, the phase-change heat dissipation and system EER are at their maximum when the heat exchanger has three processes. In comparison to two processes, the heat dissipation increases by 7% to 16.7%. In contrast, when compared to four processes, the heat dissipation increases by 5.1% to 7.2%. The EER relative to two processes increased by 3.9% to 10.3%, while relative to four processes, it increased by 7.4% to 12.7%. This indicates that when employing a heat exchanger for phase-change cooling of fuel cells, the number of heat exchanger processes must be taken into account.
- At the same heat exchanger processes, increasing the fan speed can enhance the system heat dissipation. However, this results in a gradual decrease in the EER, with a reduction ranging between 2.9% and 30.2%. This demonstrates the substantial influence of fan power on the system EER, indicating that merely increasing the fan speed may not necessarily result in enhanced heat dissipation. Moreover, a moderate increase in the working fluid-flow rate can enhance both the system's heat dissipation and the EER. Nevertheless, the rate of improvement gradually diminishes, suggesting that the optimal working fluid-flow rate should be determined based on specific requirements.

Acknowledgment

This work is supported by Longitudinal Project, Henan Province Science and Technology Tackling Key Problems Project (202102310556)

References

[1] Crew, B., Solving the energy crisis, *Nature, 609* (2022), Sept., S1
[2] Manisalidis, I., *et al.*, Environmental and Health Impacts of Air Pollution: A Review, *Frontiers in Public Health*, *8* (2020), 14
[3] He, C. H., *et al.*, Controlling the Kinematics of a Spring-Pendulum System Using an Energy Harvesting Device, *Journal of Low Frequency Noise, Vibration & Active Control, 41* (2022), 13, pp. 1234-1257

[4] Chen, Z. J., *et al.*, Balancing Volumetric and Gravimetric Uptake in Highly Porous Materials for Clean Energy, *Science*, *368* (2020), 6488, pp. 297-303
[5] Fang, X. M., Li, X. L., Design and Simulation of Hybrid Thermal Energy Storage Control for Photovoltaic Full Cells, *Thermal Science*, *27* (2023), 2A, pp.1031-1039
[6] Zeng, H., *et al.*, Development and Prospect of Fuel Cell Technology for Distributed Power System, *Power Generation Technology*, *39* (2018), 2, pp. 165-170
[7] Faghri, A., Guo, Z., Challenges and Opportunities of Thermal Management Issues Related to Fuel Cell Technology and Modeling, *International Journal of Heat and Mass Transfer*, *48* (2005), Sept., pp. 3891-3920
[8] Shao, Z., *et al.*, Hydrogen Energy and Fuel Cell Development Status and Outlook, *Bulletin of Chinese Academy of Sciences*, *34* (2019), 4, pp. 469-477
[9] Qin, Y., *et al.* Research Progress on Cooling System for Proton Exchange Membrane Fuel Cell Stack, *Automobile Technology*, *59* (2021), 11, pp. 1-14
[10] Kandlikar, S. G., Lu, Z., Thermal Management Issues in a PEMFC Stack – A Brief Review of Current Status, A*pplied Thermal Engineering*, *29* (2009), 7, pp. 1276-1280
[11] Tong, Z., *et al.*, Thermal Control of Fuel Cell Engine Stack, *Chemical Industry and Engineering Progress*, *34* (2015), 8, pp. 3009-3014
[12] Zhao, J., Thermal Performance Enhancement of Air-Cooled Proton Exchange Membrane Fuel Cells by Vapor Chambers, *Energy Convers Manage*, *213* (2020), 112830
[13] Zheng, W., *et al.*, Simulation and Experimental Study on Thermal Management System of Vehicle Fuel Cell, *Automotive Engineering*, *43* (2021), 3, pp. 381-386
[14] Ding, Y., *et al.*, Characteristic Analysis of Heat Transfer and Pressure Drop on Fuel Cell Engine Radiator, *Chinese Journal of Power Sources*, *38* (2014), 2, pp. 262-264+275
[15] Tao, L., *et al.*, Proton Exchange Membrane Fuel Cell Vehicle Auxiliary Heat Dissipation System Design Modeling and Analysis, *Acta Energiae Solaris Sinica*, *44* (2023), 4, pp. 299-305

Paper submitted: December 12, 2023
Paper revised: May 15, 20244
Paper accepted: May 15, 2024